International Journal of Material and Mechanical Engineering, 2012, 1: 1-7
Published Online April 2012

http://www.ijm-me.org

Using Fiber Reinforced Polymer to Restore Deteriorated Structural Members

W. K. Ahmed[1], A-H. I. Mourad[2]
[1]Engineering Requirements Unit, Faculty of Engineering, United Arab Emirates University, UAE
[2]Mechanical Engineering Department, Faculty of Engineering, United Arab Emirates University, UAE
Email: w.ahmed@uaeu.ac.ae

(Abstract) The objective of this work is to investigate the effect of using FRP strengthening techniques to rehabilitate cracked structural members like beams under numerous loading conditions. Liner Elastic Fracture Mechanics was adopted in this research program in order to estimate Mode I Stress Intensity Factor (SIF). Standard FEM (ANSYS) was used to simulate the cracked beams by using 8-node quadrilateral element. The current analysis showed that SIF of the cracked structural member decreases by using FRP laminate because of crack bridging. In addition length, thickness and fiber volume fraction of the FRP has great influence on decreasing the estimated SIF.
Keywords: crack; deteriorated; FEM; FRP; restore; SIF.

1. INTRODUCTION

Many steel structural members are in need for rehabilitation because they may suffer fatigue cracking or corrosion damage. Strengthening may also be required due to increase in their weights, and there is a demand to increase the flexural capacity of these members. The repair of the structural members by FRP rehabilitation techniques is one of the promising retrofit and common techniques. This is metallic due to its ease of application and the weight added to a structure is minimal. The cracks could propagate and cause complete failure of the member. The use of Fiber Reinforced Polymer (FRP) sheets to repair the cracked members could be a quite encouraging technique because replacing the whole structure could be very costly. This may contribute labor savings and reducing requirements for staging and lifting materials. Traditional procedures for strengthening and rehabilitation of damaged steel structures often require welding or bolting of the structure. In contrast the fatigue performance of bonded composite of cracked steel members has been shown to be effective up to 20 million cycles [1]. It has also been estimated that bonded carbon fiber reinforced polymers CFRP strips have been used over 10000 times for the repair of corrosion and fatigue damage of aircrafts [2]. These effects illustrate the increasing acceptance of such technique in applications where safety and durability are the criteria. The goal of this research is to restore the strength of the cracked members, and this was investigated numerically by FEM. A parametric study is intended to demonstrate the effectiveness of a proposed repair technique for cracked structural members by using FRP batches. Using standard Finite Element (FE) program ANSYS [3], has simulated the cracking in the structural, members and the element used in the analysis is 8-node quadrilateral element. Three types of beams were investigated under various loading conditions and the numerically estimated Stress Intensity Factor (SIF) was calculated by using Liner Elastic Fracture Mechanics (LEFM) technology in order to neglect the crack tip plasticity [4, 5].

2. BACKGROUND

Linear elastic fracture mechanics technology is based on an analytical procedure that relates the stress field magnitude and distribution in the vicinity of a crack tip to the nominal stress applied to the structural member, size, shape and orientation of the crack and material properties [4]. The fundamental principle of the fracture mechanics is that the stress field a head of a sharp crack in structural member can be represented by a single parameter K, (SIF) that has a unit of $MN.m^{-3/2}$. This parameter relates both the nominal stress level σ in the member and the size of the crack present a .Paris and Sih [4] showed that in order to establish methods of stress analysis for cracks in elastic solid, it is convenient to define three types of relative movement of two crack surfaces. These displacement modes represent the local deformation in an infinitesimal element containing a crack front which is the opening mode, mode I, the sliding or shear mode, mode II and the tearing mode, mode III .It is clear that each of these modes of deformation corresponds to a basic type of stress field in the vicinity of crack tips. In any case the deformations at the crack tip can be treated as one or combined of these local displacement modes. Moreover the stress field at the crack tip can be treated as one or a combination of the three basic types

of stress fields. Most practical design situations and failures correspond to mode I, which is the mode, considered in this study.

Westergaared and Irwin [4] developed a method to show that the stress and displacement field in the vicinity of crack tip for a linear, elastic, homogeneous, and isotropic solid subjected to the three modes of deformation are given by:

$$\sigma_x = \frac{K_I}{\sqrt{2\pi r}}\cos(\theta/2)[1-\sin(\theta/2)\sin(3\theta/2)] \quad (1)$$

$$\sigma_y = \frac{K_I}{\sqrt{2\pi r}}\cos(\theta/2)[1+\sin(\theta/2)\sin(3\theta/2)] \quad (2)$$

$$\tau_{xy} = \frac{K_I}{\sqrt{2\pi r}}\cos(\theta/2)\sin(\theta/2)\cos(3\theta/2) \quad (3)$$

$$u = \frac{K_I}{2G}\sqrt{\frac{r}{2\pi}}\cos(\theta/2)[k-1+2\sin^2(\theta/2)] \quad (4)$$

$$v = \frac{K_I}{2G}\sqrt{\frac{r}{2\pi}}\sin(\theta/2)[k+1-2\cos^2(\theta/2)] \quad (5)$$

where,

K_I is stress intensity factor for mode I .

G = Shear modulus = E/2(1+μ)

k=(3-μ)/(1+μ) for plane stress

k=3-4μ for plane strain

μ= Poisson's ratio

σ_z=0 for plane stress

σ_z=μ(σ_x-σ_y) for plane strain

It may be stated that most brittle fractures occur under conditions of mode I loading [6], therefore the stress of primary intent and in most practical applications is σ_y .The stress becomes infinite and the SIF is then a measure of the stress singularity at the crack tip. For σ_y to be a maximum in **Eq.2**, let θ=0°, therefore:

$$\sigma_y = \frac{K_I}{\sqrt{2\pi r}} \Rightarrow K_I = \sigma_Y\sqrt{2\pi r} \quad (6)$$

It is clear that at location far from crack tip, σ_y decreases, and K_I remains constant and describes the intensity of the stress field just ahead of sharp crack.

3. CASES STUDIED

A simply supported beam of length=400mm, width=40mm and thickness =40mm, as shown in **Figure 1**. The beam is subjected to shear force of 5.5kN which represent 20% of the yield stress of the structural steel AISI 1020, is the case study one. While the same geometry of the beam under a tensile load, as shown in **Figure 2**, is the case study two. It is assumed that the beams were made of steel with Young's modulus of E=200*10^3 MPa and Poisson's ratio of μ=0.3. The investigation includes the study of SIF for both unstrengthened and strengthened cracked beam for the two cases. The crack depth of a=4mm, 8mm, 12mm, 16mm and 20mm were studied. These values are corresponding to crack length to width ratio a/W of 0.1, 0.2, 0.3, 0.4 and 0.5 respectively. The effect of stiffener dimensions on SIF, thickness t (20mm, 40mm and 80mm) and length L (8mm, 20mm) were considered Fig.3 and 4. In addition a comparison is made to investigate the effect of using different types of the fiber reinforcement (i.e. fiber glass, kevlar and carbon fiber) of different modulus of elasticity. This is to explore the effect of stiffener stiffness.

4. FINITE ELEMENT MODELING

The numerical modeling for all cases was based on the finite element method FEM by using two dimensional plain strain 8-node quadrilateral element (Solid 86) [3] in ANSYS and is used to obtain well established singular stress field by shifting the mid-nodes one-quarter away from crack tip to compute SIF. Because of symmetry, only one half of the beam was modeled and all models were meshed with the same degree of refinement at the crack edge to obtain consistent result. The finite element boundary condition of the cracked beam is shown in **Figure 5** and **6**, while the boundary conditions for the strengthened cracked beam are shown in **Figure 7** and **8**. The typical FE mesh adopted in the analysis is shown in **Figure** 9.

5. STRENGTHENING MATERIAL

Three different types of fiber reinforced epoxy composite stiffeners are used in the study. These are fiber glass, kevlar and carbon fibers. **Table 1** [7] show a comparison for the modulus of elasticity of three types. The modulus of elasticity and the Poisson's ratio of the used bonding adhesive (Epoxy) is 3.5GPa μ=0.25 respectively. This is according to the data sheet provided by the manufacturers [8]. Because of the complexity of the problem investigated, the FRP batch was assumed to be isotropic for each of the materials.

The composite modulus of elasticity computed by using the following relation [6]:

$$E_c=E_fV_f+E_mV_m \quad (7)$$

where E_c, E_f and E_m are the modulus of elasticity of composite batch, fiber and matrix respectively, and V_f and V_m are the volume fraction of the fiber and matrix respectively. The volume fraction of the fibers used 25%, 50% and 75%. **Table 2** shows the effect of V_f on the composite stiffener modulus of elasticity calculated using **Eq.**7.

6. ESTIMATING OF SIF BY FEM

Fracture mechanics generally is based on two types of analysis [10], namely residual strength analysis to determine the maximum crack size that can be tolerated, and fatigue crack growth analysis to calculate the time for crack growth from a certain initial crack size until the maximum tolerable crack size in order to determine the safe life. These analyses are usually based on the SIF intensity factor. Therefore, knowing the SIF is important for the fracture mechanics. Stress intensity factor can always be expressed as:

$$K = \sigma\sqrt{\pi a}\ \mathrm{Y} \qquad (8)$$

where *Y* is a dimensionless factor which depends upon geometry of the body and crack size. The problem resides in the determination of *Y*. Solutions of *Y* for many configurations have been obtained. Compilations of these solutions known as stress intensity factor handbook [11] are available. Components that contain cracks may be subjected to one or more different types of load, such as uniform tensile loads, concentrated tensile loads, or bending loads. In such a case the total SIF can be found by algebraically adding the SIF that corresponds to each load if it is available. This method is known as the superposition method [10]. It can be noted that superposition is the addition of SIF and not of *Y*. The value of *Y* of each case has to be obtained separately and SIF calculated separately and then added [10]. Many structural configurations are so complicated, that a solution may not be available in handbooks. Consequently the finite element method was and still a powerful tool to determine crack tip stress fields. By finite element solution a complicated engineering geometry could be analyzed, also it has been extensively used in engineering crack problems, such as the determination of SIF.

Basically there are two different approaches to determine SIF by the finite element method [10]. One is the direct method in which SIF is calculated from stress field or from displacement field. The second is an indirect method in which SIF is calculated from other parameter, the line integral (*J*-Integral). In this study the direct method is considered. The displacement method involves a correlation of the finite element nodal point displacements with the well-known crack tip displacement equation. For mode I, the crack tip displacement **Eq.4** and **5** can be written as:

$$\cup_i = \frac{K_I}{2G}\sqrt{\frac{r}{2\pi}}\ f_i(\theta) \qquad (9)$$

where U_1=u and U_2=v

$f_1 = \cos(\theta/2)[k-1+2\sin^2(\theta/2)]$ and

$f_2 = \sin(\theta/2)[k+1-2\cos^2(\theta/2)]$

By substituting a nodal point displacement U_i at some point (r,θ) near the crack tip into **Eq.9** a quantity K_I can be calculated as:

$$K_I = \sqrt{\frac{2\pi}{r}}\frac{2G\cup_i}{f_i(\theta)} \qquad (10)$$

From plots of K_I as a function of *r* for fixed values of θ and a particular displacement component, estimates of K_I can be made. If the exact theoretical displacement is substituted in **Eq.10** then value of K_I obtained as *r* approaches zero would be the exact value of K_I. Since the finite element displacements are rather inaccurate at an infinitesimal distance from the crack tip, this process is not useable. Instead a tangent extrapolating of the K_I curve is used to estimate K_I [12]. With suitable refinement of element size the K_I curves obtained from element displacements rapidly approach a constant slope with increasing distance (*r*) from the crack tip.

The estimation of the SIF by the tangent extrapolating method could be made by plotting a tangent line to the constant slope portion of the curve and extending the line until an intersection with K_I is obtained at point, which is the estimated value of K_I. The most accurate estimates are obtained from K_I curve corresponding to the normal displacement on the crack surface at θ=180° [10], hence **Eq.10** is therefore can be written:

$$K_I = \frac{2Gv}{f_2(180^o)}\sqrt{\frac{2\pi}{r}} \qquad (11)$$

The stress method for determining the crack tip SIF involves a correlation of the finite element nodal stresses with the well-known crack tip stress equations.

For mode I, the crack tip stress, **Eq.1**, **2** and **3** can be written as:

$$\sigma_{ij} = \frac{K_I}{\sqrt{2\pi r}}\ f_{ij}(\theta) \qquad (12)$$

where $\sigma_{11}=\sigma_{xx}$, $\sigma_{22}=\sigma_{yy}$, $\sigma_{12}=\sigma_{xy}$

$f_{11} = f_{xx} = \cos(\theta/2)[1-\sin(\theta/2)\sin(3\theta/2)]$

$f_{22} = f_{yy} = \cos(\theta/2)[1+\sin(\theta/2)\sin(3\theta/2)]$

$f_{12} = f_{xy} = \cos(\theta/2)\sin(\theta/2)\cos(3\theta/2)$

Nodal point stresses σ_{ij} in the vicinity of the crack tip can be substituted into **Eq.12** and values of K_I can be calculated from:

$$K_I = \frac{\sqrt{2\pi r}}{f_{ij}(\theta)}\sigma_{ij} \qquad (13)$$

The estimation of SIF could be made by plotting K_I as a function of *r* for fixed value of θ and a particular stress component. If the exact theoretical stresses are substituted into **Eq.13** then the intercept of the curve with the K_I axis at r=0 would be the exact value of K_I. Due to the inability of the finite element method to represent the stress singularity conditions at the crack tip, the K_I curve for *r* greater than zero must again be extrapolated back to r=0 The extrapolated value of K_I at r = 0 is the estimated K_I.

Accurate evaluation of the SIF by stress method could be obtained from plotting K_I curve corresponding to the normal stress on the crack tip (σ_y) at angle θ=0° [13]. Hence **Eq.13** can be written:

$$K_I = \sigma_Y\frac{\sqrt{2\pi r}}{f_Y(0^o)} \qquad (14)$$

7. ESTIMATING OF SIF BY FEM

Figure 10 shows the normalized reduction in SIF using different batch geometries under bending condition. The V_f of the reinforced batch was chosen to be 25%, which is the common V_f value for hand lay-up process. The commonly used V_f range is approximately 30-40%. Whereas with the higher quality, more sophisticated and precise processes are used in the aerospace industry, V_f approaching 70% can be successfully obtained [14]. Accordingly, a range of V_f from 25% up to 75% is adopted for the batch reinforcement specification. **Table** 3 demonstrates the percentage reduction for each batch dimension for a crack depth a/W=(0.1, 0.2, 0.3, 0.4 and 0.5).It

is observed that the maximum drop in SIF is 77% , whereas the optimum batch chosen for subsequent analysis was t=0.2W, L=0.5W for economic consideration. For stiffened cracked beam subjected to tensile load, the results are shown in **Figure** 11, where normalized SIF is shown. The percentage reduction of SIF is shown in **Table** 4, where the maximum drop in SIF is 60%. Again due to cost-effective concern, an optimum geometry was chosen analogous to the chose dimensions for bending (t=0.2W, L=0.5W). Therefore these dimensions are adopted for the subsequent analysis. The effect of the variation of V_f on SIF is represented by **Figure** 12, and its percentage of reduction of SIF is obvious in **Table** 5. It is concluded that V_f=25% is reasonable for rehabilitation, although, pre-preg strips can be used to add more stiffness. Using different types of fibers, the impact on the SIF is shown in **Figure 13** and the percentage drop in SIF is presented in **Table 6**. This is for the flexural loading case. Although carbon fiber showed the highest reduction, but this is due to its higher stiffness. The effect of using different V_f and different types of fibers for tensile case are shown in **Figure 14** and **15**, which are explained by the **Table 7** and 8.It is clear that the maximum reduction in SIF by was 56% for V_f=75%, whereas the reduction was 67% for the carbon fiber stiffener of V_f=25%.

8. CONCLUSION

The FE technique is used to estimate mode I SIF of cracked beam for both tensile and bending load. The following conclusions illustrate a summary of the results:

1. Fiber volume fraction of 25% is the major reduction in SIF, although 50%-75% showed more reduction in SIF, but is not significant.
2. For economical point of view V_f=25% is recommended since the reduction in the SIF using higher V_f has small effect in the SIF.
3. Glass fiber reinforced stiffener demonstrated a proper stiffness to be utilized for the rehabilitation of cracked beams in term of cost effective technique and to avoid the corrosive galvanic effect between carbon and the steel.

REFERENCES

[1] B.Andrea,A.Nussaumer,and M.A.Hirt."Fatique life extension of riveted bridge members using presstresed carbon fiber components".steel structures of the 2000's,ECCS,Istanbul,september 11-13.pp.375-380.

[2] H.Aglan, Q.Y.Wang and M.Kehoe."Fatique behaviour of bonded composite repair".Journal of adhesion Science and technology.V.15,n.13,2001,pp.1621-1634.

[3] S.Moaveni," Finite Element Analysis ,theory and application with ANSYS",Printice Hall,Inc.,1999.

[4] D.Broeck," The practical use of fracture mechanics" ,Kulmer Acadimic Publishers,1988

[5] J.M.Barsom," Fracture and Fatigue control in structure ",Prentice-Hall,Inc.,1987.

[6] H.L Edwards, R.J.H.Wanhill,"Fracture mechanics", Edward Arnold, 1989

[7] G.Eckold," Design and manufacture of composite structures ",McGraw-Hill,Inc.,1994.

[8] N.G.McCrum, Principle of Polymers Engineering,1997.

[9] R. M. Jones ," Mechanics of composite materials ",1975

[10] D.Broek, "Elementary engineering fracture,"Martinus Nijhoff publishers, 1987.

[11] Stress intensity factor handbook,vol.1&vol.2,Pergamon Press,1987

[12] S.K. Chan,"On the finite element method in linear fracture mechanics", Engineering fracture mechanics, Vol.2p.p1, 1970.

[13] C.F.shih," Crack extension modeling with quadratic isoparametric element", International Journal of Fracture,12,1976.

[14] M.M.Shwartz, "Composite Materials Handbook", McGraw-Hill company, 1984.

Table 1.MODULUS OF ELASTICITY FOR DIFFERENT FIBERS

Modulus of Elasticity GPa				
Epoxy	**E-Glass**	**Kevlar**	**Steel**	**Carbon**
3.5	76	124	205	640

Table 2. FRP'S MODULUS OF ELASTICITY VERSUS VF%

Modulus of Elasticity GPa			
V_f%	**E-Glass**	**Kevlar**	**Carbon**
25	21.6	33.6	162.6
50	39.75	63.7	321.7
75	57.87	93.87	480

TABLE 3.PERCENTAGE REDUCTION OF SIF USING DIFFERENT BATCH GEOMETRY, VF=25%, BENDING

a/W	**t=0.2W L=0.5W**	**t=0.2W L=W**	**t=0.2W L=2W**	**t=0.5W L=W**	**t=0.5W L=2W**
0.1-0.5	24-65%	28-69%	29-70%	31-71%	41-77%

Table 4.PERCENTAGE REDUCTION OF SIF USING DIFFERENT BATCH GEOMETRY, VF=25%, TENSION

a/W	**t=0.2W L=0.5W**	**t=0.2W L=W**	**t=0.2W L=2W**	**t=0.5W L=W**	**t=0.5W L=2W**
0.1-0.5	30-50%	31-51%	32-52%	34-54%	38%-60%

Table 5.PERCENTAGE REDUCTION IN SIF USING DIFFERENT VF RATIO(GLASS FIBER), BENDING CASE

a/W	**V_f=25%**	**V_f=50%**	**V_f=75%**
0.1-0.5	24-65%	30-68%	34-70%

Table 6.PERCENTAGE REDUCTION OF SIF BY USING DIFFERENT TYPES OF FIBERS(VF=25%), BENDING CASE

a/W	**Glass fiber**	**Kevlar**	**Carbon**
0.1-0.5	24-65%	29-69%	50-77%

Table 7.PERCENTAGE REDUCTION IN SIF USING DIFFERENT VF RATIO(GLASS FIBER), TENSILE CASE

a/W	**V_f=25%**	**Vf=50%**	**V_f=75%**
0.1-0.5	30-50%	34-53%	38-56%

Table 8.PERCENTAGE REDUCTION OF SIF BY USING DIFFERENT TYPES OF FIBERS(VF=25%), TENSILE CASE

a/W	Glass fiber	Kevlar	Carbon
0.1-0.5	30-50%	35-53%	53-67%

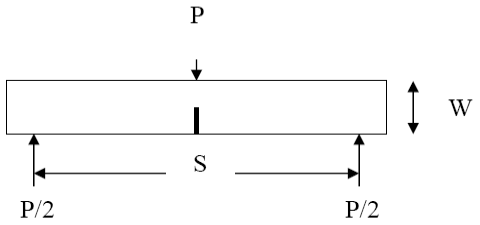

Figure 1. Cracked beam subjected to bending load.

Figure 2. Cracked beam subjected to tensile force.

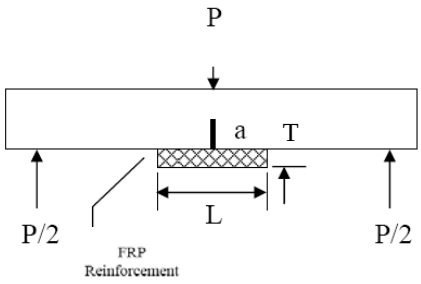

Figure 3. Cracked strengthen beam subjected to bending load.

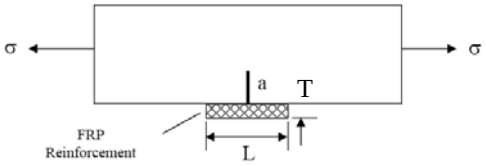

Figure 4. Cracked strengthened beam subjected to tensile load.

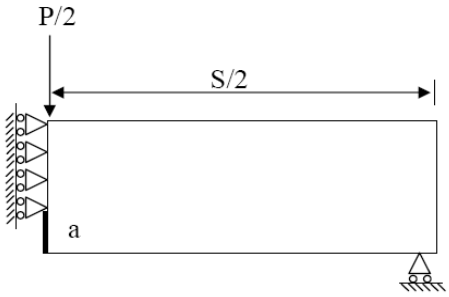

Figure 5. FE simulation of the half length of cracked beam subjected to bending force.

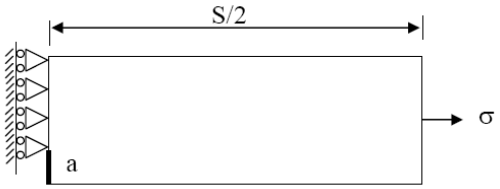

Figure 6. FE simulation of the half length of a cracked beam subjected to tensile load.

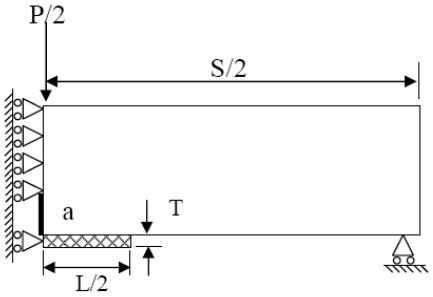

Figure 7. FE simulation of the half length of cracked strengthened beam subjected to bending force.

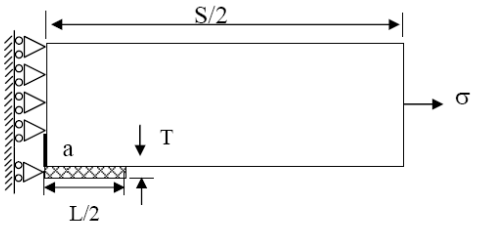

Figure 8. FE simulation of the half length of a cracked strengthened beam subjected to tensile load.

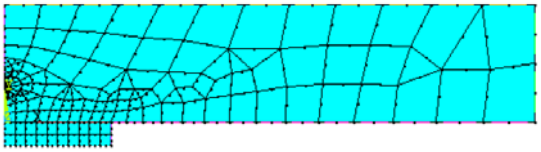

Figure 9. FE mesh of the half length of a cracked strengthened beam.

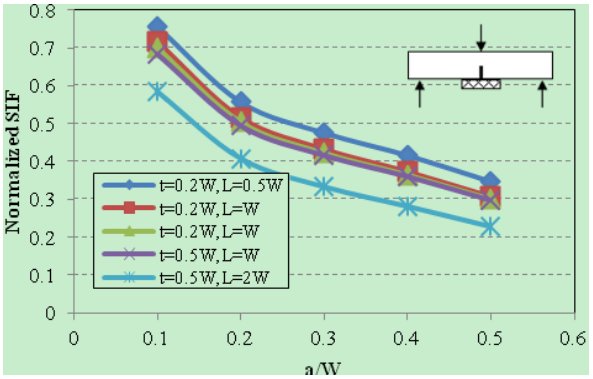

Figure 10. Variation of SIF with the reinforcement length L and thickness T.

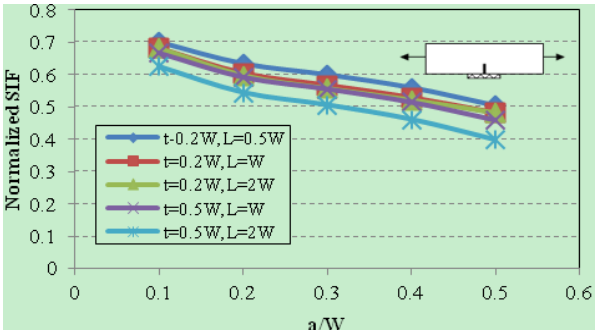

Figure 11. Variation of SIF with the reinforcement length L and thickness T.

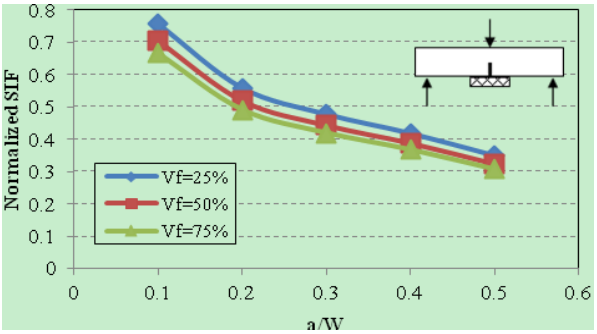

Figure 12. Effect of V_f% on SIF.

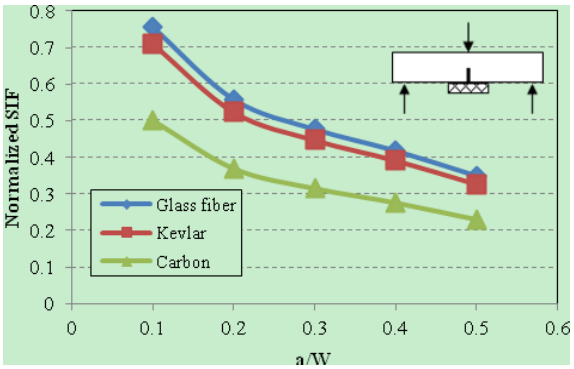

Figure 13. Variation of SIF by fibers type (V_f=25%).

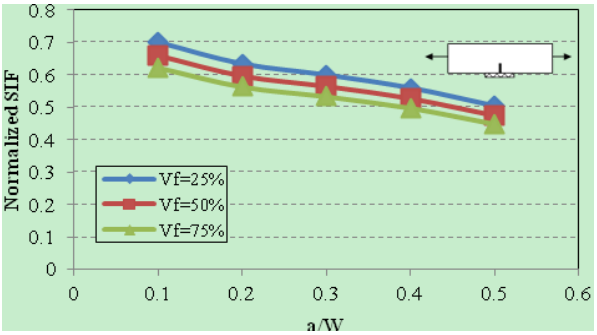

Figure 14. Effect of V_f% on SIF.

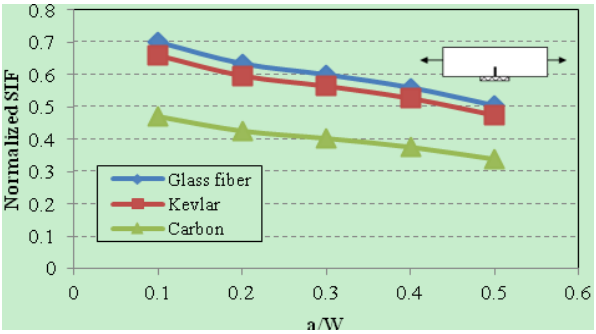

Figure 15. Variation of SIF by fibers type (V_f=25%).